

Current Biology

***FLOWERING LOCUS T* paralogs control the annual growth cycle in *Populus* trees**

Highlights

- *Populus* trees contain several paralogs of *FLOWERING LOCUS T (FT)* genes
- The *FT* paralogs regulate different aspects of the tree's yearly growth cycle
- The *FT2* paralogs control summer growth
- The *FT1* paralog controls the release of winter dormancy

Authors

Domenique André, Alice Marcon, Keh Chien Lee, ..., Nicolas Delhomme, Markus Schmid, Ove Nilsson

Correspondence

ove.nilsson@slu.se

In brief

André et al. show that in *Populus tremula* trees, a pair of *FLOWERING LOCUS T (FT)* paralogs are required for vegetative growth during spring and summer and regulate the entry into winter dormancy. Another paralog is required for bud flush in spring. This function is linked to the release of dormancy rather than to the regulation of bud flush per se.



Report

FLOWERING LOCUS *T* paralogs control the annual growth cycle in *Populus* trees

Domenique André,¹ Alice Marcon,¹ Keh Chien Lee,¹ Daniela Goretti,^{1,3} Bo Zhang,¹ Nicolas Delhomme,¹ Markus Schmid,² and Ove Nilsson^{1,4,*}

¹Umeå Plant Science Centre, Department of Forest Genetics and Plant Physiology, Swedish University of Agricultural Sciences, 901 83 Umeå, Sweden

²Umeå Plant Science Centre, Department of Plant Physiology, Umeå University, 907 36 Umeå, Sweden

³Present address: Umeå Plant Science Centre, Department of Plant Physiology, Umeå University, 907 36 Umeå, Sweden

⁴Lead contact

*Correspondence: ove.nilsson@slu.se

<https://doi.org/10.1016/j.cub.2022.05.023>

SUMMARY

In temperate and boreal regions, perennials adapt their annual growth cycle to the change of seasons. These adaptations ensure survival in harsh environmental conditions, allowing growth at different latitudes and altitudes, and are therefore tightly regulated. *Populus* tree species cease growth and form terminal buds in autumn when photoperiod falls below a certain threshold.¹ This is followed by establishment of dormancy and cold hardiness over the winter. At the center of the photoperiodic pathway in *Populus* is the gene *FLOWERING LOCUS T2* (*FT2*), which is expressed during summer and harbors significant SNPs in its locus associated with timing of bud set.^{1–4} The paralogous gene *FT1*, on the other hand, is hyper-induced in chilling buds during winter.^{3,5} Even though its function is so far unknown, it has been suggested to be involved in the regulation of flowering and the release of winter dormancy.^{3,5} In this study, we employ CRISPR-Cas9-mediated gene editing to individually study the function of the *FT*-like genes in *Populus* trees. We show that while *FT2* is required for vegetative growth during spring and summer and regulates the entry into dormancy, expression of *FT1* is absolutely required for bud flush in spring. Gene expression profiling suggests that this function of *FT1* is linked to the release of winter dormancy rather than to the regulation of bud flush per se. These data show how *FT* duplication and sub-functionalization have allowed *Populus* trees to regulate two completely different and major developmental control points during the yearly growth cycle.

RESULTS AND DISCUSSION

Populus species have several *FT* genes

The *Populus FT1* and *FT2* paralogs are the result of the salicoid whole-genome duplication event.⁶ A more local *FT2* duplication event has been described in European aspen (*Populus tremula*),⁴ but the functional relevance is so far unknown. From here on, we will refer to the duplicated *FT2* genes as *FT2a* and *FT2b*, where *FT2a* corresponds to the previously characterized *FT2* gene. A 500 kb introgression event in the genome region harboring *FT2a* and *FT2b* was recently shown to be strongly associated with local adaptation.^{4,7} Phylogenetic analysis revealed that *FT2a* and *FT2b* are present in *Populus tremula*, *P. tremuloides*, and *P. trichocarpa*, indicating that the duplication took place before the species separated (Figures 1A and S1A). We then compared the gene synteny, the genomic regions surrounding the *FT*-like genes in *Arabidopsis*, *P. tremula*, and *P. trichocarpa* (Figure 1A). Orthologous genes have a similar arrangement in all three species. The duplication around *FT2* seems to have included the orthologous gene of *FASCIATA1* (*FAS1*). However, in *P. trichocarpa* both *FT2b* and *FAS1* are truncated, while both genes are full length in *P. tremula* (Figure 1A).

Expression patterns of *FT2* genes are similar but different from *FT1*

The expression patterns of *FT1* and *FT2a* have previously been established,³ but nothing was known about *FT2b*. Thus, we analyzed the expression of all three *FT* genes in our model species T89 (*Populus tremula* × *tremuloides*) as well as in field-grown mature *Populus tremula* (Figures 1B–1D). In our samples, *FT2a* and *FT2b* expression was limited to leaves in long days. *FT2b* was significantly more highly expressed than *FT2a* (Figures 1B and 1C), but both followed a circadian rhythm with a peak at the end of the light period (Figure 1B), similar to *Arabidopsis FT*.⁸ *FT2b* overexpression also induced a dramatic early flowering phenotype (Figures S1B and S1C) similar to what has been reported for *FT1* and *FT2a*.^{1,2} *FT1*, on the other hand, was exclusively expressed in buds exposed to cold temperatures (Figures 1C and 1D). In these buds, *in situ* hybridization revealed that the transcript is broadly present in shoot apex, embryonic leaves, and vasculature in February, but is undetectable in May (Figure S1D).

FTs are required for vegetative growth

Previous attempts to study the role of individual *FT* genes in *Populus* trees have been hampered by the fact that due to high levels



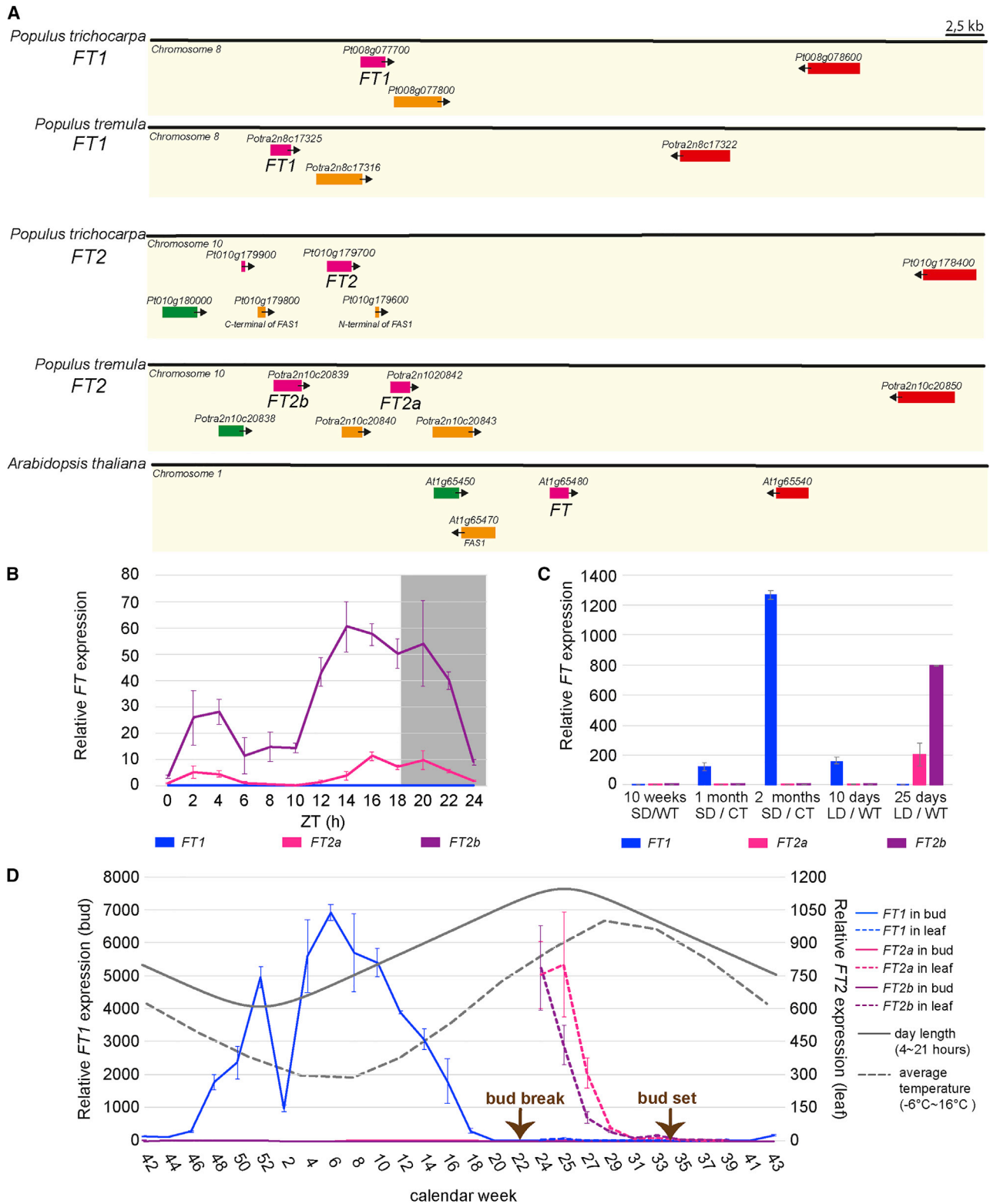


Figure 1. *Populus* FT genes are the result of both a whole-genome and a local duplication event and are expressed at different times in different tissues

(A) Genome organization of FT genes in *Arabidopsis thaliana*, *Populus trichocarpa*, and *Populus tremula*. A first salicoid whole-genome duplication created the paralogs FT1 and FT2. A second local duplication created FT2a and FT2b, the latter being truncated in *P. trichocarpa*. Orthologous genes are indicated by the same colors.

(legend continued on next page)

of homology it has been impossible to generate gene-specific knockdowns using RNAi or artificial microRNAs. To understand their individual roles, we generated specific knockout mutants for *FT1* and *FT2* using CRISPR-Cas9 (Figures S2A and S2B) and subjected the mutant plants to a simulation of the changing seasons to examine their phenotypes (Figure 2). *FT2* has previously been identified as an important regulator of the timing of bud set since RNAi-mediated downregulation of *FT* expression leads to earlier bud set while *FT* overexpression prevents growth cessation and bud set.¹ SNPs at the *FT2a* locus are also very strongly associated with timing of bud set in *Populus tremula*.⁴ However, surprisingly, knockout of *FT2a* expression had no visible effect on vegetative growth or timing of growth cessation/bud set (Figure S2C). In contrast, knockout of *FT2b* expression had a clear effect leading to bud set already in long day conditions (Figure S2D). However, a much more dramatic phenotype was seen in *FT2a FT2b* double knockouts, which displayed a severely dwarfed phenotype because of bud set even in tissue culture under 23-h-long days, and immediately after transplanting to soil (Figures 2A and 2E), suggesting that the *FT2* genes are necessary to maintain vegetative growth. While *FT2b* appears to have the most important function, presumably linked to higher levels of expression compared to *FT2a*, the genes are partially redundant. A similarly extreme phenotype has been shown for *GIGANTEA (GI)* RNAi plants, which display very low *FT2* expression.⁹ However, in contrast to *GI* RNAi trees, *FT2* double-knockout plants were not impaired in their bud flush (Figure 2D), suggesting that the *FT2* genes have specific roles in the maintenance of vegetative growth and in the regulation of growth cessation and bud set. Recently, it was shown that CRISPR knockouts of *FT2a* lead to early growth cessation and inhibition of elongation growth in *P. tremula × alba*.¹⁰ Since the presence of the active *P. tremula* gene *FT2b* reported here was not known at that time, the retention of this active gene likely explains the relatively weaker phenotypes reported in these CRISPR lines compared to our double *ft2a ft2b* lines.

While RNAi-mediated downregulation of *FT2* expression had already hinted at their function,¹ only preliminary data regarding the phenotypes of *ft1* and *ft1 ft2* trees have been described.¹¹ In our experiments, disruption of *FT1* function using CRISPR-Cas9 had no visible effect on vegetative growth or SD-induced growth cessation (Figure 2), confirming that the gene has no function during these processes when it is not expressed (Figures 1B–1D). However, after cold treatment to break dormancy and reactivation at warmer temperatures, *ft1* plants were unable to flush their buds and only some plants flushed a few buds several months later (Figures 2B–2D and 2F). This is a similar but stronger phenotype than the previously described preliminary data in

Populus tremula × alba.¹¹ To exclude the possibility of *ft1* buds simply having died during the cold treatment, we performed a viability staining, which showed that buds were indeed still alive (Figure S4A). This shows that *FT1* is required to resume vegetative growth after winter. Together, these results show that both *FT1* and *FT2* are required for vegetative growth: *FT1* is required for bud flush and *FT2* is required to allow vegetative growth and prevent growth cessation and bud set during summer.

FT2 is graft transmissible while FT1 function is restricted to its place of production

We also investigated whether grafting on T89 could rescue the growth defect of *FT* CRISPR plants (Figure S3). *FT* is a mobile graft-transmissible protein in Arabidopsis^{12–14} and has recently been shown to also be a long-ranged signal in poplar.¹⁵ We grafted both *ft1* and *ft2a ft2b* scions onto wild-type (WT) rootstocks, as well as WT scions on mutant rootstocks. The early growth cessation of *ft2a ft2b* plants could be temporarily rescued (Figure S3A) by a WT rootstock. However, as the shoot grew the WT rootstock could no longer support the growth of the *ft2a ft2b* scion, and it went into growth cessation again. Conversely, WT scions initially grew slowly on *ft2a ft2b* rootstock but then started to grow normally, presumably because they were now able to produce enough *FT2* themselves, which in Arabidopsis typically occurs when leaves turn from photosynthate sinks to sources.¹⁶

Grafting of *ft1*, however, did not rescue the delayed bud flush phenotype (Figure S3B). WT parts of the grafts flushed simultaneously as the WT control regardless of their position. *ft1* scions, rootstocks, and controls did not flush during the entirety of the experiment. These results indicate that *FT1* is acting locally within individual buds. Since *FT1* is expressed in embryonic leaves and vasculature (Figure S1D) and has also been shown to be mobile, it is still possible that *FT1* travels locally to the embryonic shoot apex, as suggested earlier.⁵

FT1 is required for dormancy release

Since dormancy release is a prerequisite for bud flush, it is very difficult to know in which of these interconnected processes *FT1* has a role, especially since there are no well-established molecular markers for dormancy release.¹⁷ We therefore performed transcript profiling on WT and *ft1* buds at different time points during an artificial growth cycle (Figure 3) to see at what point in time lack of *FT1* expression affected the transcriptome. The analysis showed that the transcriptomes of *ft1* mutant plants look like those of WT controls up until 4 weeks of cold treatment (CTW4) (Figure 3A). After 8 weeks (CTW8), when WT endodormancy is released, the WT had drastically changed its transcriptomic profile, while *ft1* seemed to remain in the same stage as at

(B) Relative gene expression of *FT1*, *FT2a*, and *FT2b* in leaves of WT trees grown for 2 months in a greenhouse under 18 h light, 6 h dark regime. Error bars indicate SEM of six biological replicates (ramets).

(C) Relative gene expression of *FT1*, *FT2a*, and *FT2b* in buds as well as in leaves of newly flushing buds (25 days LD/WT) of WT grown in growth chamber. Lateral buds were harvested at ZT6. Plants were grown for 6 weeks in LD conditions before being subjected to the indicated treatments. SD/WT, short day and warm temperature treatment (20°C, 8 h light/16 h dark); SD/CT, short day and cold temperature treatment (4°C, 8 h light/16 h dark); LD/WT, long day and warm temperature treatment (20°C, 18 h light/6 h dark). Error bars indicate SEM of three biological replicates (ramets).

(D) Expression of *FT1*, *FT2a*, and *FT2b* over the course of 1 year in field-grown *P. tremula* in Umeå, Sweden. *FT1* expression peaked during winter, when temperatures were lowest. Both *FT2* genes were expressed in leaves during summer months. Solid lines indicate expression in apical buds; dashed line expression in leaves. All samples were taken at 2 p.m. In each panel, gene expression is normalized against the lowest detectable *FT1* and *FT2a* expression in buds and leaves, respectively. Error bars indicate SEM of three biological replicates.

See also Figure S1.

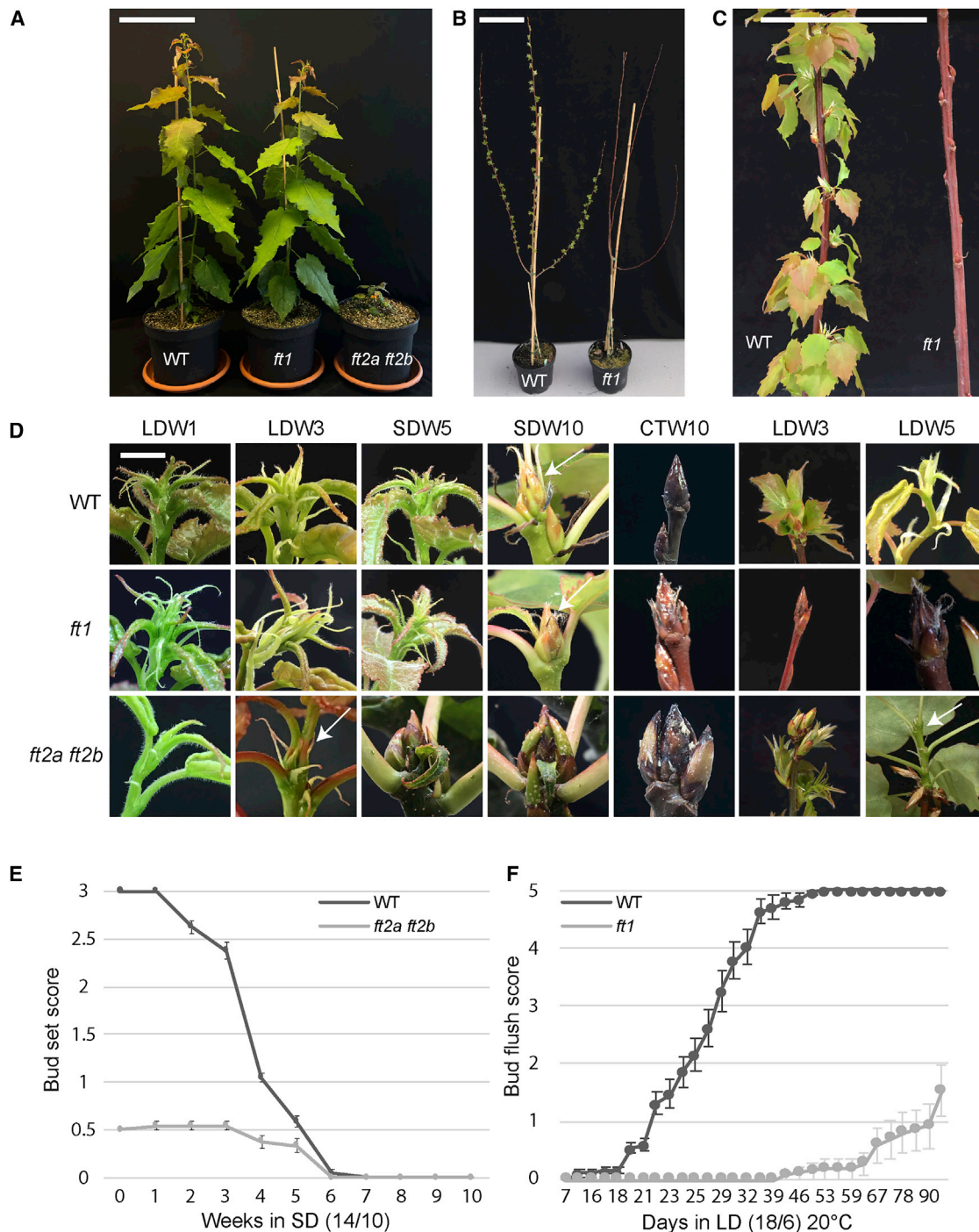


Figure 2. *FT1* and *FT2* are required for growth at different times

(A) WT, *ft1*, and *ft2a ft2b* mutants after 4 weeks in LD. *ft2a ft2b* mutants are severely dwarfed.

(B) WT and *ft1* trees after 3 weeks in warm LD following 10 weeks of cold treatment at 4°C.

(C) Close-up of WT and *ft1* shoots after 4 weeks in warm LD following 10 weeks of cold treatment at 4°C.

(D) Shoot apices over the course of one growth cycle of WT, *ft1*, and *ft2a ft2b* trees. Knockout of *FT1* had no effect on bud set, while *ft2a ft2b* double mutant lines set bud already in LD. White arrows indicate bud formation stages. Bud flush after cold was not impaired in *ft2a ft2b*, but severely delayed (if occurring at all) in *ft1* trees. LDW, weeks in LD (18/6 h light/dark, 20°C/20°C); SDW, weeks in SD (14/10 h light/dark, 20°C/20°C); CTW, weeks in cold treatment (8/16 h light/dark, 4°C/4°C).

(legend continued on next page)

CTW4 (Figures 3A and 3B; Data S1A–S1F). This is also represented in the number of differentially expressed genes between WT and mutant trees at the different time points (Figure 3C; Data S1G–S1I). After 7 days of warm temperature (LDD7; just before any visible signs of bud flush), the transcriptomes were again more similar, presumably due to a similar response to the temperature increase and the fact that bud flush had not yet started. The most affected Gene Ontology (GO) terms were “catalytic activity” for genes downregulated in WT between CTW4 and CTW8, and that remained high in *ft1* versus WT at CTW8, and “binding” and metabolic process for genes with the opposite pattern of expression (Data S1G–S1I). A closer examination of the expression of genes previously suggested to be associated with the regulation of dormancy or bud set/bud break showed the most consistent changes between WT and *ft1* at CTW8 in genes associated with GA metabolism and reception (Figure 3D). In particular, the GA receptor *GIBBERELLIN-INSENSITIVE DWARF (GID)* genes are upregulated in WT at CTW8 while they are maintained at lower expression levels in *ft1*, suggesting a possible role for GA reception in the release of dormancy. Also, *PICKLE (PKL)*, an antagonist of polycomb repression complex 2 whose downregulation has been shown to mediate the ABA-induced plasmodesmata closure and establishment of dormancy in *Populus* trees,¹⁸ is induced in WT at CTW8 while it remains low in *ft1*, suggesting a possible involvement in dormancy release (Figure 3D). It can be speculated that the very large number of genes changing in expression during dormancy release could be indicative of a more general chromatin remodeling releasing a repressed state of a large number of genes. The role of FT1 would then be to release the repressed state and make the genes accessible for later inductive signals.

Our data suggest that *FT1* function is required for dormancy release rather than bud flush per se. This was further supported by moving WT and *ft1* trees with non-dormant buds back to long days before dormancy was established. Under these conditions, both WT and *ft1* trees flushed their buds normally (Figure S4B), showing that *FT1* is only required for bud flush after dormancy release. However, we cannot exclude that *FT1* also has a role in post-dormancy-specific bud flush.

Since dormancy release occurs at a similar time as removal of plasmodesmata callose plugs,⁵ we wondered how FT1 influences this process. After 12 weeks of short days, both WT and *ft1* trees were dormant and had developed frequent electron-dense plasmodesmata callose plugs, or dormancy sphincters, in apices (Figures 4A and 4C), as shown before.¹⁸ After a further 12 weeks of cold treatment, when WT dormancy has been released while *ft1* trees are still dormant, no plasmodesmata callose plugs could be found in either WT or *ft1* (Figures 4B and 4D). This shows that FT1 has no role in the removal of the callose plugs but is rather acting downstream of or parallel to this process. It also shows that it is not the removal of the callose plugs per se that determines the dormant versus non-dormant state. One possibility is that a local movement of FT1 to target cells

in the shoot apex is absolutely required to release dormancy, and that the dormancy sphincters are needed to prevent this movement. However, it is still unclear to what extent opening of the dormancy sphincters is required for dormancy release after cold treatment, or if it is just a consequence of that release. Also, at the peak of its expression FT1 displays a broad expression in the shoot apex, in vasculature, and in the young leaf primordia (Figure S1), making it unclear if a restriction of FT1 movement is relevant. A better understanding of direct FT1 targets is required to better understand the mechanism for dormancy release. Taken together, these data show that FT1 is required for dormancy release and the concomitant bud flush, even though its specific mode of action remains unknown.

Taken together, our data show that *FLOWERING LOCUS T* genes are indispensable for the correct regulation of the annual growth cycle, being critical both for the growth arrest and bud set in the fall and for bud flush in the spring, i.e., the start and stop of the growing season. They evolved from a whole-genome duplication, but despite their sub-functionalization, they still share a common role as growth promoters and are able to induce a shared set of genes when ectopically expressed.³ As a consequence, both *FT1* and *FT2* ectopic overexpression leads to early flowering and prevention of growth cessation.^{1–3} This suggests that the sub-functionalization is primarily driven by changes in the regulatory elements of the two genes, leading to completely contrasting expression patterns. This is reminiscent of the situation in sugar beet where two *FT* paralogs have evolved complementary expression patterns to regulate the yearly growth cycle. However, in this case there is also a neo-functionalization leading to one of the paralogs acting as a repressor instead of an activator of flowering.^{19,20} Despite the previous focus on *FT2a*, it seems that in *Populus tremula* × *tremuloides*, *FT2b* can act redundantly in promoting growth and is of even greater relative importance, since knockout of any *FT2* alone led to no (*ft2a*) or a slight (*ft2b*) growth phenotype (Figures S2C and S2D) while double knockout almost completely prevented growth by an immediate trigger of the SD response (Figure 2).

There are now several examples of how sub-functionalized *FT* paralogs have evolved within different species to regulate completely different aspects of plant development and growth, usually in response to photoperiodic cues. This includes, for instance, the regulation of flowering and tuberization in potato,²¹ bulb formation in onion,²² and short-day vernalization providing competence to flower in *Brachypodium*.²³ Besides the regulation of flowering, *FT* homologs also appear to act as general growth regulators in tomato²⁴ and maize.²⁵

Interestingly, recent work has shown that *Gentiana trifolia*, a herbaceous perennial, has two *FT* genes where one gene is expressed during the growing season to regulate flowering while the other is expressed in underground overwintering buds to release them from dormancy.²⁶ CRISPR knockouts of this latter gene lead to a reduced frequency of, and delay in, bud break. This is a very similar situation to what we have shown in *Populus*

(E) Bud set score of WT and *ft2a ft2b* trees in SD. Scores describe the transition from active growth (3) to a fully developed bud (0). Error bars indicate SEM of 15 biological replicates.

(F) Bud flush score of WT and *ft1* trees after cold treatment. Scores describe the transition from hard, closed buds (0) to fully opened buds and actively growing apices (5). Error bars indicate SEM of ten biological replicates.

See also Figures S2 and S3.

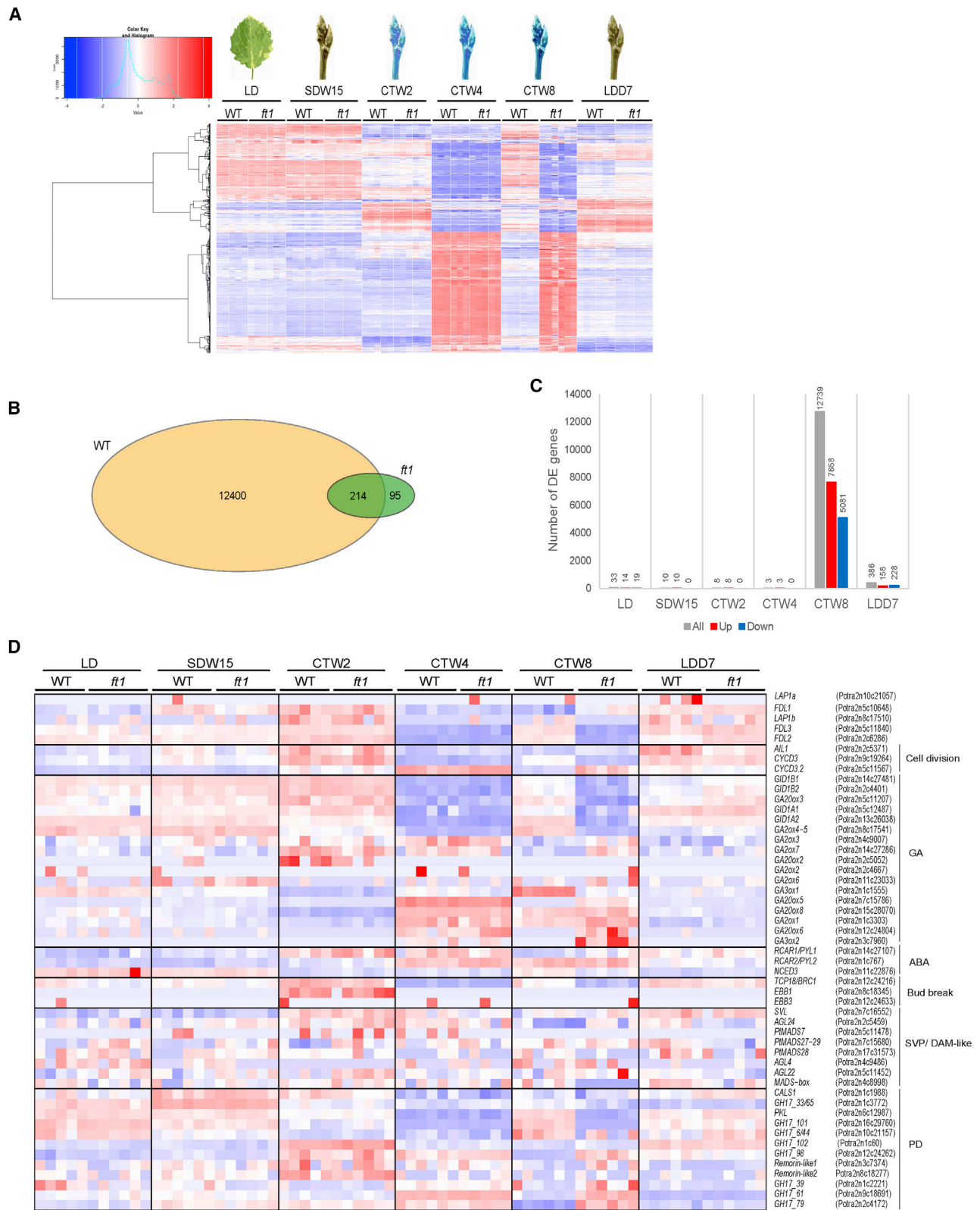


Figure 3. Differential gene expression in *ft1* trees during a growth and dormancy cycle

(A) Heatmap for all time points of WT and *ft1* samples from six biological replicates.

(B) Venn diagram comparing the number of differentially expressed (DE) genes between CTW4 and CTW8 in WT and *ft1*.

(legend continued on next page)

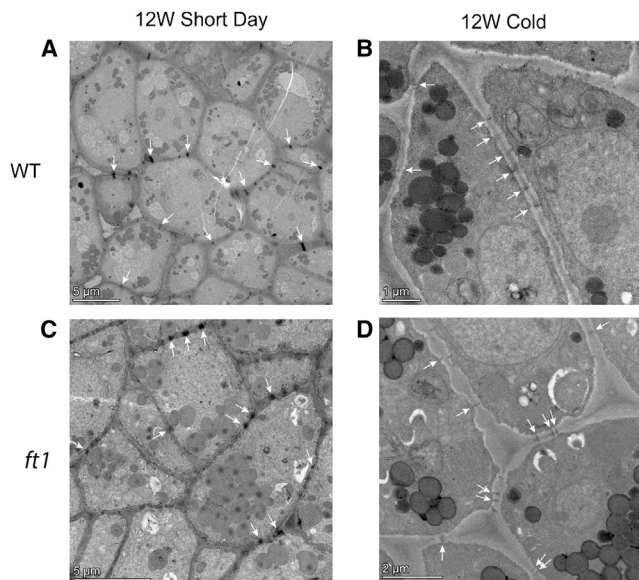


Figure 4. *ft1* shoot apices lack plasmodesmata callose plugs after cold treatment

(A and B) TEM micrographs of shoot apices in terminal buds of WT trees after 12 weeks in SD (A) followed by 12 weeks of chilling (B).

(C and D) TEM micrographs of shoot apices in terminal buds of *ft1* trees after 12 weeks in SD (C) followed by 12 weeks of chilling (D).

Both WT and *ft1* apices display frequent electron-dense plasmodesmata callose plugs in dormancy sphincters (arrows) after 12 weeks in short day (A and C), while no callose plugs are found in plasmodesmata (arrows) after cold treatment (B and D).

See also Figures S3 and S4.

trees and suggests that this type of *FT* sub-functionalization and control of dormancy release might be a more general feature of perennial plants.

Although *FT1* has previously been suggested to be the *FT* paralog controlling flowering,³ the situation in poplar is clearly different from the one in Arabidopsis. *FT1* is not expressed in leaves and seems to be under no circadian control. Furthermore, it is specifically induced by low temperatures, which repress *FT* expression in Arabidopsis.²⁷ It is not known which transcription factors activate *FT1* expression. SHORT VEGETATIVE PHASE-LIKE (SVL) has been shown to attenuate its induction,²⁸ but simple downregulation of a repressor seems insufficient to explain the *FT1* hyper-induction. Our data clearly show that *FT1* has another function, besides potentially flowering, in promoting vegetative growth after winter. To what extent *FT1* and *FT2* are actually needed to control flowering remains an open question.

Taken together, we show here that the *FT* paralogs in *Populus* trees have sub-functionalized to control major developmental transitions during the annual growth cycle, being required to prevent

premature growth cessation and bud set in the fall and to induce bud flush in the spring, most likely by releasing the trees from winter dormancy. These are all critical aspects in a tree's ability to adapt to growth in different climates such as those experienced at different latitudes and altitudes, or as a result of climate change.

STAR★METHODS

Detailed methods are provided in the online version of this paper and include the following:

- KEY RESOURCES TABLE
- RESOURCE AVAILABILITY
 - Lead contact
 - Materials availability
 - Data and code availability
- EXPERIMENTAL MODEL AND SUBJECT DETAILS
- METHOD DETAILS
 - Plant material and growth conditions
 - Design and cloning of CRISPR constructs
 - Design and cloning of *35S_{pro}:FT2b-GFP*
 - Generation of CRISPR-Cas9 lines
 - Grafting experiments
 - RNA extraction and quality assessment
 - Quantitative real-time PCR
 - RNA sequencing analysis
 - Pre-processing of RNA-Seq data and differential expression analyses
 - *In situ* hybridization
 - Viability staining
 - Transmission electron microscopy
- QUANTIFICATION AND STATISTICAL ANALYSIS

SUPPLEMENTAL INFORMATION

Supplemental information can be found online at <https://doi.org/10.1016/j.cub.2022.05.023>.

ACKNOWLEDGMENTS

This work was supported by grants from the Swedish Research Council, the Knut and Alice Wallenberg Foundation, Kempe Foundation, and the Swedish Governmental Agency for Innovation Systems (VINNOVA). We thank SNIC/Uppsala Multidisciplinary Center for Advanced Computational Science for assistance with massively parallel sequencing and access to the UPPMAX computational infrastructure. We also thank Agnieszka Ziolkowska and the Umeå Core Facility for Electron Microscopy (UCEM) for help with electron microscopy.

AUTHOR CONTRIBUTIONS

D.A., M.S., and O.N. planned the research. D.A., K.C.L., D.G., A.M., B.Z., and N.D. performed the experiments and analyzed the data. D.A. and O.N. wrote the manuscript. All authors reviewed and approved its final version.

(C) Number of DE genes between WT and *ft1* trees at the individual time points.

(D) Heatmap for all time points of WT and *ft1* samples of genes previously suggested to be associated with the regulation of dormancy or bud set/bud break. GA, genes involved in gibberellin metabolism and reception; ABA, genes involved in ABA metabolism and reception; PD, genes suggested to be associated with callose synthesis and degradation during plasmodesmata callose plug formation and removal.

LD, long day; SDW15, 15 weeks in SD (14 h light/10 h dark); CTW, weeks in cold treatment (8/16 h light/dark, 4°C/4°C); LDD7, 7 days after transfer back to warm temperatures (18/6 h light/dark, 20°C/20°C). LD samples were leaves taken at ZT17.5; SDW15-LDD7 were lateral buds taken at ZT6. See also Data S1 and Figure S3.

DECLARATION OF INTERESTS

The authors declare no competing interests.

Received: February 8, 2022

Revised: April 13, 2022

Accepted: May 10, 2022

Published: June 3, 2022

REFERENCES

- Böhlenius, H., Huang, T., Charbonnel-Campaa, L., Brunner, A.M., Jansson, S., Strauss, S.H., and Nilsson, O. (2006). CO/FT regulatory module controls timing of flowering and seasonal growth cessation in trees. *Science* 312, 1040–1043. <https://doi.org/10.1126/science.1126038>.
- Hsu, C.-Y., Liu, Y., Luthe, D.S., and Yuceer, C. (2006). Poplar FT2 shortens the juvenile phase and promotes seasonal flowering. *Plant Cell* 18, 1846–1861. <https://doi.org/10.1105/tpc.106.041038>.
- Hsu, C.-Y., Adams, J.P., Kim, H., No, K., Ma, C., Strauss, S.H., Drnevich, J., Vanderveide, L., Ellis, J.D., Rice, B.M., et al. (2011). FLOWERING LOCUS T duplication coordinates reproductive and vegetative growth in perennial poplar. *Proc. Natl. Acad. Sci. USA* 108, 10756–10761. <https://doi.org/10.1073/pnas.1104713108>.
- Wang, J., Ding, J., Tan, B., Robinson, K.M., Michelson, I.H., Johansson, A., Nystedt, B., Scofield, D.G., Nilsson, O., Jansson, S., et al. (2018). A major locus controls local adaptation and adaptive life history variation in a perennial plant. *Genome Biol.* 19, 1–17. <https://doi.org/10.1186/s13059-018-1444-y>.
- Rinne, P.L., Welling, A., Vahala, J., Ripel, L., Ruonala, R., Kangasjärvi, J., and van der Schoot, C. (2011). Chilling of dormant buds hyperinduces FLOWERING LOCUS T and recruits GA-inducible 1, 3- β -glucanases to reopen signal conduits and release dormancy in Populus. *Plant Cell* 23, 130–146. <https://doi.org/10.1105/tpc.110.081307>.
- Tuskan, G.A., DiFazio, S., Jansson, S., Bohlmann, J., Grigoriev, I., Hellsten, U., Putnam, N., Ralph, S., Rombauts, S., Salamov, A., et al. (2006). The genome of black cottonwood, *Populus trichocarpa* (Torr. & Gray). *Science* 313, 1596–1604. <https://doi.org/10.1126/science.1128691>.
- Rendón-Anaya, M., Wilson, J., Sveinsson, S., Fedorkov, A., Cottrell, J., Bailey, M.E.S., Rupis, D., Lexer, C., Jansson, S., Robinson, K.M., et al. (2021). Adaptive introgression facilitates adaptation to high latitudes in European aspen (*Populus tremula* L.). *Mol. Biol. Evol.* 38, 5034–5050. <https://doi.org/10.1093/molbev/msab229>.
- Suárez-López, P., Wheatley, K., Robson, F., Onouchi, H., Valverde, F., and Coupland, G. (2001). CONSTANS mediates between the circadian clock and the control of flowering in Arabidopsis. *Nature* 410, 1116–1120. <https://doi.org/10.1038/35074138>.
- Ding, J., Böhlenius, H., Rühl, M.G., Chen, P., Sane, S., Zambrano, J.A., Zheng, B., Eriksson, M.E., and Nilsson, O. (2018). GIGANTEA-like genes control seasonal growth cessation in populus. *New Phytol.* 218, 1491–1503. <https://doi.org/10.1111/nph.15087>.
- Gómez-Soto, D., Allona, I., and Perales, M. (2022). FLOWERING LOCUS T2 promotes shoot apex development and restricts internode elongation via the 13-hydroxylation gibberellin biosynthesis pathway in Poplar. *Front. Plant Sci.* 12, 814195. <https://doi.org/10.3389/fpls.2021.814195>.
- Sheng, X. (2018). Flowering gene homologs regulate seasonal growth changes in poplar. PhD thesis (Virginia Polytechnic Institute and State University).
- Corbesier, L., Vincent, C., Jang, S., Fornara, F., Fan, Q., Searle, I., Giakountis, A., Farrona, S., Gissot, L., Turnbull, C., and Coupland, G. (2007). FT protein movement contributes to long-distance signaling in floral induction of Arabidopsis. *Science* 316, 1030–1033. <https://doi.org/10.1126/science.1141752>.
- Jaeger, K.E., and Wigge, P.A. (2007). FT protein acts as a long-range signal in Arabidopsis. *Curr. Biol.* 17, 1050–1054. <https://doi.org/10.1016/j.cub.2007.05.008>.
- Mathieu, J., Warthmann, N., Küttner, F., and Schmid, M. (2007). Export of FT protein from phloem companion cells is sufficient for floral induction in Arabidopsis. *Curr. Biol.* 17, 1055–1060. <https://doi.org/10.1016/j.cub.2007.05.009>.
- Miskolczi, P., Singh, R.K., Tylewicz, S., Azeez, A., Maurya, J.P., Tarkowská, D., Novák, O., Jonsson, K., and Bhalerao, R.P. (2019). Long-range mobile signals mediate seasonal control of shoot growth. *Proc. Natl. Acad. Sci. USA* 116, 10852–10857. <https://doi.org/10.1073/pnas.1902199116>.
- Takada, S., and Goto, K. (1993). TERMINAL FLOWER2, an Arabidopsis homolog of HETEROCHROMATIN PROTEIN1, counteracts the activation of FLOWERING LOCUS T by CONSTANS in the vascular tissues of leaves to regulate flowering time. *Plant Cell* 15, 2856–2865. <https://doi.org/10.1105/tpc.016345>.
- Singh, R.K., Svystun, T., Aldahmash, B., Jönsson, A.M., and Bhalerao, R.P. (2016). Photoperiod and temperature mediated control of phenology in trees—a molecular perspective. *New Phytol.* 213, 511–524. <https://doi.org/10.1111/nph.14346>.
- Tylewicz, S., Petterle, A., Marttila, S., Miskolczi, P., Azeez, A., Singh, R.K., Immanen, J., Mähler, N., Hvidsten, T.R., Eklund, D.M., et al. (2018). Photoperiodic control of seasonal growth is mediated by ABA acting on cell-cell communication. *Science* 360, 212–215. <https://doi.org/10.1126/science.aan8576>.
- Pin, P.A., Benlloch, R., Bonnet, D., Wremerth-Weich, E., Kraft, T., Gielen, J.J.L., and Nilsson, O. (2010). An antagonistic pair of FT homologs mediates the control of flowering time in sugar beet. *Science* 330, 1397–1400. <https://doi.org/10.1126/science.1197004>.
- Pin, P., and Nilsson, O. (2012). The multifaceted roles of FLOWERING LOCUS T in plant development. *Plant Cell Environ.* 35, 1742–1755. <https://doi.org/10.1111/j.1365-3040.2012.02558.x>.
- Navarro, C., Abelenda, J.A., Cruz-Oró, E., Cuéllar, C.A., Tamaki, S., Silva, J., Shimamoto, K., and Prat, S. (2011). Control of flowering and storage organ formation in potato by FLOWERING LOCUS T. *Nature* 478, 119–122. <https://doi.org/10.1038/nature10431>.
- Lee, R., Baldwin, S., Kenel, F., McCallum, J., and Macknight, R. (2013). FLOWERING LOCUS T genes control onion bulb formation and flowering. *Nat. Commun.* 4, 1–9. <https://doi.org/10.1038/ncomms3884>.
- Woods, D., Dong, Y., Bouche, F., Bednarek, R., Rowe, M., Ream, T., and Amasino, R. (2019). A florigen paralog is required for short-day vernalization in a pooid grass. *eLife* 8, e42153. <https://doi.org/10.7554/eLife.42153>.
- Lifschitz, E., Eviatar, T., Rozman, A., Shalit, A., Goldshmidt, A., Amsellem, Z., Alvarez, J.P., and Eshed, Y. (2006). The tomato FT ortholog triggers systemic signals that regulate growth and flowering and substitute for diverse environmental stimuli. *Proc. Natl. Acad. Sci. USA* 103, 6398–6403. <https://doi.org/10.1073/pnas.0601620103>.
- Danilevskaya, O.N., Meng, X., McGonigle, B., and Muszynski, M.G. (2011). Beyond flowering time: pleiotropic function of the maize flowering hormone florigen. *Plant Signal. Behav.* 6, 1267–1270. <https://doi.org/10.4161/psb.6.9.16423>.
- Takahashi, H., Nishihara, M., Yoshida, C., and Itoh, K. (2022). Gentian FLOWERING LOCUS T orthologs regulate phase transitions: floral induction and endodormancy release. *Plant Physiol.* 188, 1887–1899. <https://doi.org/10.1093/plphys/kiac007>.
- Marín-González, E., Matías-Hernández, L., Aguilar-Jaramillo, A.E., Lee, J.H., Ahn, J.H., Suárez-López, P., and Pelaz, S. (2015). SHORT VEGETATIVE PHASE up-regulates TEMPRANILLO2 floral repressor at low ambient temperatures. *Plant Physiol.* 169, 1214–1224. <https://doi.org/10.1104/pp.15.00570>.
- Singh, R.K., Maurya, J.P., Azeez, A., Miskolczi, P., Tylewicz, S., Stojković, K., Delhomme, N., Busov, V., and Bhalerao, R.P. (2018). A genetic network mediating the control of bud break in hybrid aspen. *Nat. Commun.* 9, 1–10. <https://doi.org/10.1038/s41467-018-06696-y>.
- Koncz, C., and Schell, J. (1986). The promoter of T_L-DNA gene 5 controls the tissue-specific expression of chimaeric genes carried by a novel type

- of *Agrobacterium* binary vector. *Mol. Gen. Genet.* 204, 383–396. <https://doi.org/10.1007/bf00331014>.
30. Karimi, M., Depicker, A., and Hilson, P. (2007). Recombinational cloning with plant gateway vectors. *Plant Physiol.* 145, 1144–1154. <https://doi.org/10.1104/pp.107.106989>.
 31. Kumar, S., Stecher, G., Li, M., Niyaz, C., and Tamura, K. (2018). MEGA X: molecular evolutionary genetics analysis across computing platforms. *Mol. Biol. Evol.* 35, 1547–1549. <https://doi.org/10.1093/molbev/msy096>.
 32. Ibáñez, C., Kozarewa, I., Johansson, M., Ögren, E., Rohde, A., and Eriksson, M.E. (2010). Circadian clock components regulate entry and affect exit of seasonal dormancy as well as winter hardiness in populus trees. *Plant Physiol.* 153, 1823–1833. <https://doi.org/10.1104/pp.110.158220>.
 33. Lampropoulos, A., Sutikovic, Z., Wenzl, C., Maegele, I., Lohmann, J.U., and Forner, J. (2013). GreenGate—a novel, versatile, and efficient cloning system for plant transgenesis. *PLoS One* 8, e83043. <https://doi.org/10.1371/journal.pone.0083043>.
 34. Nilsson, O., Aldén, T., Sitbon, F., Little, C.H.A., Chalupa, V., Sandberg, G., and Olsson, O. (1992). Spatial pattern of cauliflower mosaic virus 35S promoter-luciferase expression in transgenic hybrid aspen trees monitored by enzymatic assay and non-destructive imaging. *Transgenic Res.* 1, 209–220.
 35. Chang, S., Puryear, J., and Cairney, J. (1993). A simple and efficient method for isolating RNA from pine trees. *Plant Mol. Biol. Rep.* 11, 113–116. <https://doi.org/10.1007/bf02670468>.
 36. Livak, K.J., and Schmittgen, T.D. (2001). Analysis of relative gene expression data using real-time quantitative PCR and the 2⁻ΔΔCT method. *Methods* 25, 402–408. <https://doi.org/10.1006/meth.2001.1262>.
 37. Kopylova, E., Noé, L., and Touzet, H. (2012). SortMeRNA: fast and accurate filtering of ribosomal RNAs in metatranscriptomic data. *Bioinformatics* 28, 3211–3217. <https://doi.org/10.1093/bioinformatics/bts611>.
 38. Bolger, A.M., Lohse, M., and Usadel, B. (2014). Trimmomatic: a flexible trimmer for Illumina sequence data. *Bioinformatics* 30, 2114–2120. <https://doi.org/10.1093/bioinformatics/btu170>.
 39. Sundell, D., Mannapperuma, C., Netotea, S., Delhomme, N., Lin, Y.-C., Sjödin, A., Van de Peer, Y., Jansson, S., Hvidsten, T.R., and Street, N.R. (2015). The Plant Genome Integrative Explorer Resource: PlantGenIE.org. *New Phytol.* 208, 1149–1156. <https://doi.org/10.1111/nph.13557>.
 40. Patro, R., Duggal, G., Love, M.I., Irizarry, R.A., and Kingsford, C. (2017). Salmon provides fast and bias-aware quantification of transcript expression. *Nat. Methods* 14, 417–419. <https://doi.org/10.1038/nmeth.4197>.
 41. Huber, W., Carey, V.J., Gentleman, R., Anders, S., Carlson, M., Carvalho, B.S., Bravo, H.C., Davis, S., Gatto, L., Girke, T., et al. (2015). Orchestrating high-throughput genomic analysis with Bioconductor. *Nat. Methods* 12, 115–121. <https://doi.org/10.1038/nmeth.3252>.
 42. Love, M.I., Huber, W., and Anders, S. (2014). Moderated estimation of fold change and dispersion for RNA-seq data with DESeq2. *Genome Biol.* 15, 550. <https://doi.org/10.1186/s13059-014-0550-8>.
 43. Ewels, P., Magnusson, M., Lundin, S., and Käller, M. (2016). MultiQC: summarize analysis results for multiple tools and samples in a single report. *Bioinformatics* 32, 3047–3048. <https://doi.org/10.1093/bioinformatics/btw354>.

STAR★METHODS

KEY RESOURCES TABLE

REAGENT or RESOURCE	SOURCE	IDENTIFIER
Bacterial and virus strains		
<i>E. coli</i> strain: DH5a	N/A	N/A
Agrobacterium strain: GV3101	Koncz et al. ²⁹	N/A
Chemicals, peptides, and recombinant proteins		
MS basal salts	Duchefa Biochemie	Cat#M0221.0050
T4 DNA ligase	ThermoFisher Scientific	Cat#EL0011
Eco31I	ThermoFisher Scientific	Cat#ER0291
Hexadecyltrimethylammonium bromide (CTAB)	MERCK	Cat#52367
Fluorescein diacetate (FDA)	Sigma-Aldrich	Cat# F7378
Critical commercial assays		
RNeasy mini kit	QIAGEN	Cat# 74106
iScript cDNA Synthesis Kit	Bio-Rad	Cat#170-8891
SsoAdvanced Universal SYBR Green Supermix	Bio-Rad	Cat#1725270
SuperScript II Reverse Transcriptase	ThermoFisher Scientific	Cat#18064014
AMPure XP beads	Beckman-Coulter	Cat#A63882
Deposited data		
Raw and analyzed data	ENA: https://ebi.ac.uk/ena	PRJEB46745
Experimental models: Organisms/strains		
Hybrid aspen (<i>Populus tremula x tremuloides</i>) clone T89 (wild-type/WT)	N/A	N/A
<i>Populus tremula</i>	Umeå, Sweden	N/A
Oligonucleotides		
See Table S1	N/A	N/A
Recombinant DNA		
pK2GW7	Karimi et al. ³⁰	N/A
pK7GWIWG2 (I)	Karimi et al. ³⁰	N/A
pGreenGateFT1 CRISPR-CAS9	In this paper	N/A
pGreenGateFT2a CRISPR-CAS9	In this paper	N/A
pGreenGateFT2b CRISPR-CAS9	In this paper	N/A
pGreenGateFT2ab CRISPR-CAS9	In this paper	N/A
Software and algorithms		
MEGAX software	Kumar et al. ³¹	https://www.megasoftware.net/

RESOURCE AVAILABILITY

Lead contact

Further information and requests for resources and reagents should be directed to and will be fulfilled by the lead contact, Ove Nilsson (ove.nilsson@slu.se).

Materials availability

All unique/stable reagents generated in this study are available from the lead contact with a completed Materials Transfer Agreement.

Data and code availability

- RNA-seq data have been deposited at the European Nucleotide Archive (ENA: <https://ebi.ac.uk/ena>) and are publicly available as of the date of publication. Accession numbers are listed in the [key resources table](#).

- Custom R scripts used for analysis of RNA-seq data are available from <https://github.com/nicolasDelhomme/PoplarFT>. The raw data is available from the European Nucleotide Archive (ENA: <https://ebi.ac.uk/ena>) under the accession number PRJEB46745
- Any additional information required to reanalyze the data reported in this paper is available from the lead contact upon request.

EXPERIMENTAL MODEL AND SUBJECT DETAILS

Hybrid aspen (*Populus tremula x tremuloides*) clone T89 was used as experimental model.

METHOD DETAILS

Plant material and growth conditions

Hybrid aspen (*Populus tremula x tremuloides*) clone T89 was used as WT control and all genetic modifications were done in this background. Plants were cultivated on ½ Murashige and Skoog medium under sterile conditions for 4 weeks or until they had rooted (max. 8 weeks). After transfer to soil, plants were grown in growth chambers in LD (18h light, 20°C/ 6h dark, 18°C) and with weekly fertilization (10 mL NPK-Rika S/plant). Illumination was from ‘Powerstar’ lamps (HQI-T 400W/D BT E40, Osram, Germany) giving an R/FR ratio of 2.9 and a light intensity of 150–200 $\mu\text{mol m}^{-2} \text{s}^{-1}$. To induce growth cessation, plants were moved to SD (14h light, 20°C/ 10h dark, 18°C) for up to 15 weeks and fertilization was stopped. For dormancy release, plants were treated with cold (8h light, 4°C/ 16h dark, 6°C) for 8–10 weeks and then transferred back to LD for bud flush. In both SD and LD, previously published bud scores³² were used to assess effects on bud development (set/flush). For year-around gene expression analysis, a ca. 40-year-old local (Umeå, Sweden) aspen tree was sampled once a month around midday (May to August leaves, buds from September to April).

Design and cloning of CRISPR constructs

Escherichia coli strain DH5 α was used for amplification of all plasmids, which were then confirmed by sequencing (Eurofins). GreenGate entry and destination vectors³³ were acquired from Addgene. Potential sgRNAs for target genes were identified with E-CRISP (<http://www.e-crisp.org/E-CRISP>). They were introduced into entry vectors by site-directed mutagenesis PCR. The final vector (containing promoter, Cas9 CDS, terminator, two sgRNAs and resistance cassette) was assembled by GreenGate reaction (150 ng of each component, 1.5 μL FastDigest buffer, 1.5 μL of 10 mM ATP, 1 μL 30U/ μL T4 ligase and 1 μL Eco31I in a 15 μL reaction) in 50 cycles of 5 min restriction/ligation at 37°C and 16°C, respectively, followed by 5 min 50°C and 5 min 80°C. All reagents were purchased from Thermo Scientific.

Design and cloning of 35S_{pro}:FT2b–GFP

To create the 35S_{pro}:FT2b–GFP fusion gene, the coding region (CDS) of *FT2b* was amplified from cDNA and cloned into the pGREEN-IIS destination vector³³ to C-terminally fuse it in frame to *GFP* under control of the 35S promoter. The final construct was transformed by electroporation into *Agrobacterium tumefaciens* and into *ft2a ft2b* mutant hybrid aspen trees. All plasmids were propagated using the *Escherichia coli* strain DH5 α and verified by sequencing. GreenGate entry and destination vectors were obtained from Addgene. Primers used for plasmid construction are listed in Table S1.

Generation of CRISPR-Cas9 lines

Vectors with different combinations of guide RNAs (Table S1) were transformed into Hybrid aspen using a standard protocol.³⁴ At least 30 individual transgenic lines from each transformation were screened for target gene deletions using PCR (Table S1; Figure S2A). For each gene (*FT1*, *FT2a* and *FT2b*) at least two independent lines with homozygous, biallelic deletions were initially characterized for growth alterations before selecting one line for deeper analysis. All deletions were confirmed to occur at, or within a few nucleotides of, the expected PAM sites. Except for the *ft2a ft2b* double mutant lines, where both genes were confirmed to be homozygously deleted, target sites in *FT2b* were sequenced in *FT2a* CRISPR constructs and vice versa to exclude “off target” effects.

Grafting experiments

Scions of soil-grown plants were grafted onto rootstocks after 4 weeks (*ft2a ft2b*) or 5 weeks (*ft1*) in the greenhouse (18h light, 20°C/ 6h dark, 18°C). Scions were between 5 and 10 cm long and had no developed leaves, while the rootstock was decapitated ca 10 cm below the apex and kept its leaves. *ft2a ft2b* grafts were kept in these conditions until the end of the experiment, while *ft1* grafts were transferred to SD (8h light, 20°C/ 16h dark, 18°C) after 5 weeks. After 10 weeks of SD treatment, plants were subjected to cold treatment as described above and returned to warm temperatures after 2 months. 5–8 plants per graft combination was used and 4 self-grafted control plants per mutant line and wild type.

RNA extraction and quality assessment

Poplar leaves were ground to fine powder, of which 100 mg were used for RNA extraction with CTAB extraction buffer³⁵ (2% CTAB, 100 mM Tris-HCl (pH 8.0), 25 mM EDTA, 2M NaCl, 2% PVP). The samples were incubated at 65°C for 2 min and extracted twice with

an equal volume of chloroform-isoamyl alcohol (24:1). Nucleic acids were precipitated at -20°C for 3 hours with $\frac{1}{4}$ volumes 10 M LiCl. Precipitate was collected by centrifugation (13000 rpm, 4°C , 20 min) and purified with RNeasy kit (Qiagen). DNase treatment was performed on-column (Qiagen). RNA integrity was confirmed either by agarose gel (for downstream qPCR) or by Bioanalyzer (Agilent) for subsequent RNA sequencing.

Quantitative real-time PCR

1000 ng RNA were used for cDNA synthesis with iScript cDNA Synthesis Kit (Biorad). The cDNA was diluted 50 times for downstream applications. Quantitative real-time PCR (qPCR) was run on a LightCycler 480 with SYBR Green I Master (Roche). All kits and machines were used according to the manufacturer's instructions. The reaction protocol started with 5 min pre-incubation at 95°C , followed by 50 cycles of amplification consisting of 10 s denaturation at 95°C , 15 s annealing at 60°C and 20 s elongation at 72°C . For the acquisition of a melting curve fluorescence was measured during the stepwise increase in temperature from 65°C to 97°C . Relative expression levels were obtained using the $2^{-\Delta\Delta\text{Cq}}$ method.³⁶ GeNorm identified *UBQ* and *18S* as the most stable reference genes. All used primers had an efficiency of >1.8 and their correct product was confirmed by sequencing. A complete list of primer sequences can be found in Table S1.

RNA sequencing analysis

For RNA sequencing experiments RNA was isolated as described above and purified with RNeasy kit (Qiagen) according to the manufacturer's instructions. DNase treatment was performed on column (Qiagen). Concentration and quality of RNA were assessed using Qubit RNA BR Assay Kit (Invitrogen) and Bioanalyzer (Agilent), respectively. $3\ \mu\text{g}$ total RNA with RIN ≥ 8 was sent for sequencing to SciLife Lab, Stockholm. Library preparation was carried out with an Agilent NGS Bravo workstation in 96-well plates with TruSeq Stranded mRNA kit (Illumina) according to the manufacturer's instructions. mRNA was purified through selective binding to poly dT-coated beads and fragmented using divalent cations under elevated temperature. cDNA was synthesized using SuperScript II Reverse Transcriptase (ThermoFisher Scientific), cleaned with AMPure XP solution (ThermoFisher Scientific), 3' adenylated and ligated to adapters. Fragments were cleaned with AMPure XP beads (ThermoFisher Scientific), amplified by PCR and purified with AMPure XP beads (ThermoFisher Scientific). After washing with 80% ethanol, they were eluted in EB (Qiagen). The quality and concentration of the adapter-ligated libraries were checked on the LabChip GX/HT DNA high sensitivity kit and by Quant-iT, respectively. The libraries were then sequenced using the Illumina NovaSeq-6000 platform, generating from 20 to 110 million paired-end reads (2×150 bp) per sample.

Pre-processing of RNA-Seq data and differential expression analyses

The data pre-processing was performed as described here: <http://franklin.upsc.se:3000/materials/materials/Guidelines-for-RNA-Seq-data-analysis.pdf>. The quality of the raw sequence data was assessed using FastQC (<http://www.bioinformatics.babraham.ac.uk/projects/fastqc/>). Residual ribosomal RNA (rRNA) contamination was assessed and filtered using SortMeRNA (v2.1³⁷; settings-log -paired_in -fastx-sam -num_alignments 1) using the rRNA sequences provided with SortMeRNA (rfam-5s-database-id98.fasta, rfam-5.8s-database-id98.fasta, silva-arc-16s-database-id95.fasta, silva-bac-16s-database-id85.fasta, silva-euk-18s-database-id95.fasta, silva-arc-23s-database-id98.fasta, silva-bac-23s-database-id98.fasta and silva-euk-28s-database-id98.fasta). Data were then filtered to remove adapters and trimmed for quality using Trimmomatic (v0.39³⁸; settings TruSeq3-PE-2.fa:2:30:10 LEADING:3 SLIDINGWINDOW:5:20 MINLEN:50). After both filtering steps, FastQC was run again to ensure that no technical artefacts were introduced. Filtered reads were pseudo-aligned to v1.1 of the *P. tremula* transcripts (retrieved from the PopGenIE resource³⁹) using salmon (v1.1.0,⁴⁰ with non-default parameters -gcBias-seqBias -validateMappings) against an index containing the *P. tremula* v1.1 genome sequence as decoy. Statistical analysis of single-gene differential expression between conditions was performed in R (v4.0.0; R Core Team 2020) using the Bioconductor (v3.10⁴¹) DESeq2 package (v1.28.1⁴²). FDR adjusted p values were used to assess significance; a common threshold of 1% was used throughout. For the data quality assessment (QA) and visualization, the read counts were normalized using a variance stabilizing transformation (VST) as implemented in DESeq2. VST data are expression counts normalized for the difference in sequencing depth, adjusted to be homoscedastic (their variance is mean independent) and set on an approximate log₂ scale (VST is a heuristic that penalizes very low, i.e. uninformative, counts most). The biological relevance of the data - e.g. biological replicates similarity - was assessed by Principal Component Analysis (PCA) and other visualizations (e.g. heatmaps), using custom R scripts, available from <https://github.com/nicolasDelhomme/PoplarFT>. In this repository a technical overview of the data, in the form of a MultiQC report,⁴³ including raw and post-QC read counts and alignment rates is also available. The raw data is available from the European Nucleotide Archive (ENA: <https://ebi.ac.uk/ena>) under the accession number PRJEB46745.

In situ hybridization

Apical buds from mature *Populus tremula* trees grown in Umeå (63.8°N, 20.2°E) where collected in February 2020 and May 2020. Immediately after the removing of some external scales, tissues were fixed according to the protocol available at <https://www.its.caltech.edu/%7Eplantlab/protocols/insitu.pdf>. Tissues were embedded in paraffine. For the probe preparation, the CDS from *FT1* of *P. tremula* was cloned into pSP72 by using *XhoI* and *EcoRV* restriction sites. The T7 promoter was used to transcribe the antisense probe and the *SP6* promoter to transcribe the sense probe. Both probes were hydrolyzed to a length of about 250bp. All the steps

necessary to make the probes are described in the following protocol https://kramerlab.oeb.harvard.edu/files/kramerlab/files/in_situ_protocol_corrected-2.pdf?m=1430323911. The same protocol was also used as reference for the proper ISH experiment, with some minor changes. The hybridization temperature was set at 40°C, and the washes were performed at 50°C; for the tissue permeabilization we used 10 mg/mL of Proteinase K acting for 30 min. Sections (8 μm thick) were mounted on glycerol and visualized at Leica DMI8.

Viability staining

ft1 buds were taken 15 weeks after the end of cold treatment, stained with 3.6 μM fluorescein diacetate solution (Sigma-Aldrich) and photographed under a stereomicroscope (Leica DMI8). *ft1* buds from before cold treatment served as positive control, while the negative control was buds kept at -80°C for 3 days prior to staining.

Transmission electron microscopy

Both WT and *ft1* apical buds were collected after growth in 12 weeks of short photoperiod and subsequently 12 weeks of cold treatment. Apical bud samples from three biological replicates were then fixed overnight in 4% paraformaldehyde and 2.5% glutaraldehyde in 1 M Caccodylate buffer (pH 7.2); post-fixed for 2h in 1% OsO₄ in water, dehydrated, infiltrated and embedded in Spurr's resin (TAAB Laboratories Equipment Ltd, England). Ultra-thin sections of 70nm thickness were stained with uranyl acetate and lead citrate and examined with the Thermo Scientific Talos L120C transmission electron microscope.

QUANTIFICATION AND STATISTICAL ANALYSIS

The statistical details of experiments can be found in the corresponding Figure legends.